

Magnetic Reversal Time in Open Long Range Systems

F. Borgonovi,^{1,2} G. L. Celardo,³ B. Goncalves,⁴ and L. Spadafora¹

¹*Dipartimento di Matematica e Fisica, Università Cattolica, via Musei 41, 25121 Brescia, Italy*

²*I.N.F.N., Sezione di Pavia, Italy*

³*Instituto de Fisica, Benemerita Universidad Autonoma de Puebla, Puebla, Mexico*

⁴*Emory Univ., Atlanta USA*

(Dated: February 2, 2008)

Topological phase space disconnection has been recently found to be a general phenomenon in isolated anisotropic spin systems. It sets a general framework to understand the emergence of ferromagnetism in finite magnetic systems starting from microscopic models without phenomenological on-site barriers. Here we study its relevance for finite systems with long range interacting potential in contact with a thermal bath. We show that, even in this case, the induced magnetic reversal time is exponentially large in the number of spins, thus determining *stable* (to any experimental observation time) ferromagnetic behavior. Moreover, the explicit temperature dependence of the magnetic reversal time obtained from the microcanonical results, is found to be in good agreement with numerical simulations. Also, a simple and suggestive expression, indicating the Topological Energy Threshold at which the disconnection occurs, as a real energy barrier for many body systems, is obtained analytically for low temperature.

PACS numbers: 05.20.-y, 05.10.-a, 75.10.Hk, 75.60.Jk

I. INTRODUCTION

One dimensional toy models are widely investigated in statistical mechanics[1]. From one hand, the possibility to get analytical results represents the starting point for analyzing more physical models. On the other hand, due to their high simplicity, they allow a better understanding of the key mechanisms at the basis of important physical effects. It is the case of the Topological Non-connectivity Threshold (TNT), recently introduced and addressed in [2] and investigated in other related papers [3, 4, 5]. In these simple toy models, with a well defined classical limit two key features were introduced, anisotropy and long-range coupling. Even if acting in different ways, they are both essential to generate a significant disconnection of the Hamiltonian phase space leading to what is known in literature as breaking of ergodicity [3, 6]. While anisotropy is a common paradigm in the phenomenological models of ferromagnetism (usually introduced as on-site anisotropy barrier in microscopic models) [7], long range interactions were re-discovered quite recently, due to the development of powerful and efficient techniques[8]. Indeed, strictly speaking, a well known model for anisotropy including a $-M^2$ term in the magnetic energy[9] ($M = \sum S_i$ being the sum of all magnetic moments within a suitable domain) exactly matches an all-to-all interacting model close to what we consider here below. The role of anisotropy in finite spin systems has attracted much attention recently, following the experimental verification of ferromagnetic behavior in finite 1D systems with strong anisotropy [11], contrary to common expectation that ferromagnetic behavior is proper of macroscopic systems only. Theoretical works [12, 13], attempted to explain such ferromagnetic behavior in finite systems using microscopic models with on site anisotropy, inducing an effective energy barrier

and thus leading to large magnetic reversal times and to ferromagnetic behavior due to finite measurement time.

In this paper we take a different approach modeling both anisotropy and long-range with some suitable spin-spin interaction toy model as in [4] but, differently from there, and in order to produce results closer to real experiments, we put the system in contact with a thermal bath. Despite its simplicity, it can be easily fitted to more physical models: for instance spin systems with dipole interaction in 3-D, have both long range and anisotropic spin-spin interactions.

There are many different ways to model a thermal environment, especially when thermalization of a long range system is needed. Here we take the simplest route and assume that the environment is able to produce a Gibbs distribution for the system energies.

In [3] we have found, for isolated anisotropic systems with an easy axis of magnetization (defined as the direction of the magnetization in the ground state energy configuration) that the constant energy surface is disconnected in two regions with positive and negative magnetization along the easy axis. This disconnection occurs below a critical energy threshold which has been called Topological Non-connectivity Threshold. Since the phase space is disconnected we have exact ergodicity breaking and no dynamical trajectory can visit the whole constant energy surface, but is, instead, limited to the region in which it started. Moreover, being defined for all finite N , where N is the number of spins, the ergodicity breaking is not related to the thermodynamic limit. The Topological Non-connectivity Threshold is an example of topological singularity, well studied recently [14], and its existence has been pointed out in Ising models too[5]. Also, an experimental test of ergodicity breaking has been proposed [15].

Even if the connection between ergodicity breaking and

anisotropy has been shown to be a general one, independent of the range of interaction among the spins, long range interacting systems behave quite differently from short ones in the thermodynamic limit. This consequence has been studied in [4] where it was found that the disconnected portion of the energy spectrum remains finite in the thermodynamic limit for long-range interacting systems only, while it becomes negligible, in the same limit, for short-range interacting ones.

The plan of the paper is the following: In Sec. II, we review and extend the results obtained in Ref. [3, 4] concerning the microcanonical behavior of long range interacting systems. In Sec. III we present a detailed calculation of the density of states, using large deviation techniques, for a Mean Field Hamiltonian and we compared it for a generic long range interacting system. Finally in Sec. IV we study the magnetic reversal time in the canonical ensemble. In particular, we show how the magnetic reversal time for the open system can be obtained from that of the isolated one (a non trivial result). Also, a very simple approximation allows to interpret the E_{tnt} as a real energy barrier for many body spin systems at sufficiently low temperature.

II. THE TNT: MICROCANONICAL RESULTS

Our paradigmatic anisotropic model, with an adjustable interaction range, which presents ergodicity breaking for any N , is described by the following Hamiltonian:

$$H = J \left(\frac{\eta}{2} \sum_{i \neq j}^N \frac{S_i^x S_j^x}{r_{ij}^\alpha} - \frac{1}{2} \sum_{i \neq j}^N \frac{S_i^z S_j^z}{r_{ij}^\alpha} \right), \quad (1)$$

where S_i^x, S_i^y, S_i^z are the spin components, assumed to vary continuously; $i, j = 1, \dots, N$ label the spin positions on a suitable lattice of spatial dimension d , and r_{ij} is the inter-spin spatial separation. Each spin satisfies $|\vec{S}| = 1$ and $0 \leq \alpha < \infty$ parametrizes the range of interactions: decreasing range for increasing α , so that $\alpha = 0$ corresponds to an all-to-all interacting model (close to phenomenological anisotropic models), while $\alpha = \infty$ refers to a nearest neighbor interacting spin model. $-1 < \eta \leq 1$ parametrizes the degree of anisotropy and for $\eta = -1$ the Hamiltonian (1) does not have a single easy axis.

In Eq. (1) the constant $J > 0$ has been added in order to fix the scale of time and to describe the model as ferromagnetic.

Needless to say, this is not the most general spin Hamiltonian giving rise to a TNT, even if it can be considered the simplest non integrable Hamiltonian with a suitable energy threshold above which the phase space is divided.

The minimum energy configuration, with energy E_{min} , is attained when all spins are aligned along the Z -axis[4] which defines implicitly the easy axis of magnetization.

The phase space for $E = E_{min}$ contains only two spin configurations, parallel or anti-parallel to the Z -axis. Therefore, the phase space at the minimal energy is disconnected, due to the uniaxial anisotropy and it consists of two points only. We may ask now when and whether at a higher energy the constant energy surface is connected. To this purpose, let us define the TNT energy E_{tnt} as the minimum energy compatible with the constraint of zero magnetization along the easy axis of magnetization (hereafter we call m the magnetization along the easy axis)

$$E_{tnt} = \text{Min} \left[H \mid m \equiv \sum_i S_i^z / N = 0 \right].$$

It is clear that if $E_{tnt} > E_{min}$ the phase space will be disconnected for all energies $E < E_{tnt}$. We call this situation Topological Non-connection, and, as will become clear in a moment, its physical (dynamical as well as statistical) consequences are rather interesting. Indeed, since below the TNT the phase space is disconnected, no energy conserving dynamics can bring the system from a configuration with $m > 0$ to a configuration with $m < 0$, thus indicating an ergodicity breaking (impossibility to visit the whole energy surface).

A useful quantity measuring how large the disconnected energy region is, compared to the total energy range, can be introduced[4]:

$$r = \frac{E_{tnt} - E_{min}}{|E_{min}|}. \quad (2)$$

In [4] it has also been shown that the disconnection ratio r , for $N \rightarrow \infty$,

$$r \rightarrow \begin{cases} 0 & \text{for } \alpha \geq d \\ \text{const} \neq 0 & \text{for } \alpha < d, \end{cases} \quad (3)$$

where d is the dimension of the embedding lattice. Since this point has not been remarked in Ref. [4], let us stress here that the existence of a phase transition for $\alpha < d$ can be inferred from the finiteness of r in the thermodynamic limit. Indeed, for long range systems, in order to define the thermodynamic limit it is convenient to make the energy extensive. This can be achieved by multiplying the Hamiltonian by $N/|E_{min}|$. If we define the energy per particle, $e = E/N$, we can write:

$$e_{tnt} - e_{min} = \frac{N}{|E_{min}|} \left(\frac{E_{tnt}}{N} - \frac{E_{min}}{N} \right) \equiv r.$$

Since below e_{tnt} the most probable magnetization is for sure different from zero, then the specific energy at which the most probable magnetization is zero will be greater than the minimum energy in the thermodynamic limit, thus implying a phase transition. On the other hand, let us also notice that when $r \rightarrow 0$ neither the existence nor the absence of a phase transition can be deduced.

An estimate for the TNT was also given for $\alpha < d$ and large N . More precisely, it can be shown that[4]:

$$E_{tnt} \approx \begin{cases} 4E'_{min} - E_{min} & \text{for } \eta \geq \eta_{cr} \\ -\eta E_{min} & \text{for } \eta < \eta_{cr}, \end{cases} \quad (4)$$

where

$$\eta_{cr} \simeq 1 - 2^{\alpha/d} < 0,$$

and E'_{min} is the minimal energy for a system of $N/2$ spins. For $\eta > \eta_{cr}$ the TNT is given by the minimum of the second term in Eq. (1) under the constraint $m = 0$, while for $\eta < \eta_{cr}$ it is given by the minimum, under the same constraint, of the first term in Eq. (1). For $\eta < 0$ and finite N , there is a competition between the two different TNTs, therefore, in what follows, we will fix the anisotropy parameter $\eta = 1$. Needless to say this choice does not affect the generality of our results.

Due to the disconnection, below E_{tnt} the dynamical time of magnetic reversal is infinite while above and close to the energy threshold (for chaotic systems), it was found to diverge as a power law[3]:

$$\tau \sim \frac{1}{(E - E_{tnt})^\gamma} \sim e^{\Delta S} = \frac{P_{max}}{P_0}, \quad (5)$$

where ΔS is the entropic barrier between the most likely magnetic states. Here, $P_E(m)$ is the probability distribution of the magnetization m at fixed energy E , so that

$$P_{max} = \text{Max}_m P_E(m),$$

and $P_0 = P_E(m = 0)$.

The divergence found in [3] also shows that the phase space becomes connected at E_{tnt} , a non trivial result, which cannot be deduced from the true existence of E_{tnt} .

Another important result found in [3] is that, for all-to-all interacting spins ($\alpha = 0$), the exponent $\gamma \propto N$. This is related with the extensivity of the entropy $S(E, m) = \ln P_E(m)$ (here we set $k_B = 1$) and explain the huge metastability of such states even for small systems (say $N \sim 100$) and not necessarily close to the threshold E_{tnt} .

We numerically checked that, even for other power-law decreasing potentials in the long-range case $\alpha < d$,

- a power law divergence at E_{tnt} still occurs as given by Eq. (5);
- reversal time is still proportional to P_{max}/P_0 (same equation);
- the exponent $\gamma = N$.

In order to do that we computed $P_E(m = 0)$ and P_{max} for different systems using the Wang-Landau algorithm [22].

In Fig. 1 we show the power law divergence of P_{max}/P_0 for different α and N values. In order to improve the presentation we choose as a variable on the X -axis

$$\chi = \frac{E - E_{tnt}}{E_{stat} - E_{tnt}}, \quad (6)$$

where E_{stat} has been defined as the energy at which $P_{max} = P_0$ (that is when the probability distribution of the magnetization has a single peak). That way all curves have a common origin.

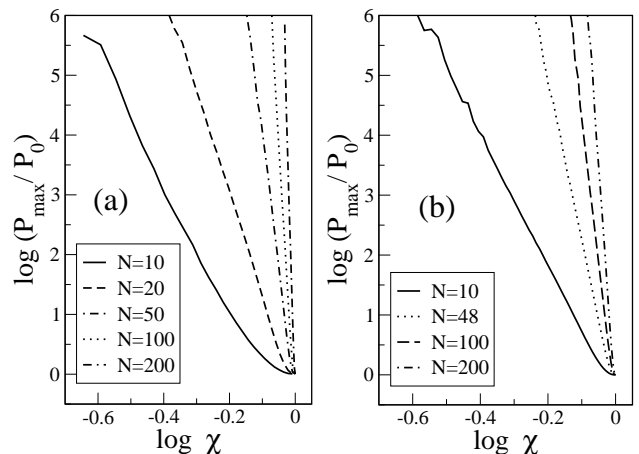


FIG. 1: $\log P_{max}/P_0$ vs $\log \chi$ for different N values as indicated in the legend and (a) $\alpha = 0.5$; (b) $\alpha = 1$.

When the isolated system has a chaotic dynamics we computed the magnetic reversal time from the direct integration of the equations of motion and we compare it with the "statistical" time P_{max}/P_0 as given by Eq. (5). We show this comparison in Fig. 2 where each point on the graph has a X coordinate P_{max}/P_0 and a Y coordinate τ . The straight lines indicated proportionality over 3 orders of magnitude.

The linear dependence $\gamma = N$ found in [3] for the case $\alpha = 0$ holds for generic α too.

In Fig. 3 we show the results of our numerical simulation for $\alpha = 0.5, 0.9, 1$. Each point γ , at fixed N has been obtained computing the statistical reversal time for different energies, as plot in Fig. 1, using the power law (5). Assuming a power law dependence $\gamma \propto N^\sigma$ we have found $\sigma \approx 1$ (within numerical errors) for all cases $\alpha \ll 1$ (we show for simplicity only the case $\alpha = 0.5$ in Fig. 3).

On the other hand, for $\alpha \sim 1$ we have numerical evidence of a slower dependence on N : $\gamma \sim N^\sigma$ with $\sigma < 1$. In the same Fig. 3 we show for sake of comparison the critical case $\alpha = d = 1$ where $\sigma = 0.78(2)$, and the close-to-critical case $\alpha = 0.9$ where we have found $\sigma = 0.87(2)$. Even if these results indicate that the simple linear relation $\gamma \propto N$ is valid for long-range interacting systems

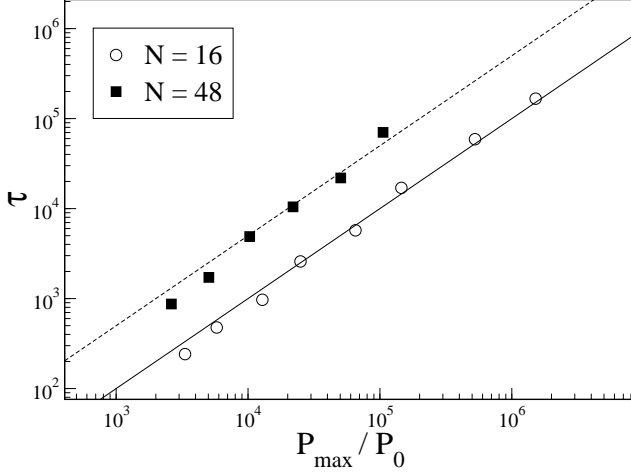


FIG. 2: Dynamical reversal time τ vs the statistical one P_{max}/P_0 for $\alpha = 1$ and different N values as indicated in the legend. Straight lines are $\tau = (1/k)P_{max}/P_0$ with $k = 10$ for $N = 16$ and $k = 2$ for $N = 48$. They have been drawn with the only purpose to guide the eye showing the proportionality between the two quantities over 3 orders of magnitude.

only, care should be used to extend the results of the case $\gamma = d = 1$ to large N since finite N effects are huge in this case. Numerical evidence for $\sigma < 1$ has also been found in the short range case ($\alpha \gg 1$) but it will be discussed elsewhere.

III. DENSITY OF STATES

The density of states (DOS) for a Mean-Field approximated Hamiltonian can be computed analytically, using large deviations techniques [24]. In particular we will show that $\rho(E) \simeq (E - E_{min})^N$ for E close to E_{min} . We will also give numerical evidence that this law still constitutes an excellent approximation of the full Hamiltonian (1) and for generic power law interaction $\alpha \neq 0$.

Let us consider the following Mean-Field Hamiltonian:

$$H_{mf} = -\frac{J}{N} \left(\sum_k S_k^z \right)^2, \quad (7)$$

which can be considered a Mean-Field approximation of the Hamiltonian (1), for low energy and $\alpha = 0$. Defining

$$m_z = \frac{1}{N} \sum_k S_k^z$$

and $e = H_{mf}/N$, Eq. (7) can be rewritten as

$$e = -Jm_z^2.$$

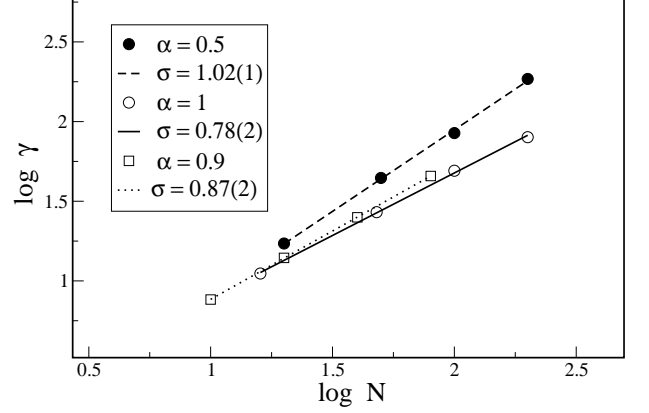


FIG. 3: $\log \gamma$ as a function of $\log N$ for different α values. Full circles stand for $\alpha = 0.5$ and dashed line is the linear fitting with slope 1.02(1). Open circles is the critical case $\alpha = d = 1$ and full line is the linear fit with slope 0.78(2). Open squares are for $\alpha = 0.9$. Standard fit procedure gives $\sigma = 0.87$ thus signaling the presence of a smooth transition at the point $\alpha = 1$ for finite N .

Let us also assume that S_k^z are random variables uniformly distributed in $[-1, 1]$.

We can compute the entropy per particle as a function of m_z using Cramer's theorem [24], so that we have:

$$s(m_z) = -\sup_{\lambda} [\lambda m_z - \ln \psi(\lambda)], \quad (8)$$

where

$$\psi(\lambda) = \langle e^{\lambda S^z} \rangle = \frac{1}{2} \int_{-1}^1 e^{\lambda S^z} dS^z = \frac{e^{\lambda} - e^{-\lambda}}{2\lambda}.$$

Taking the \sup in Eq. (8) we get:

$$\frac{\psi'(\lambda)}{\psi(\lambda)} = m_z, \quad (9)$$

which defines λ as a function of m_z . It is easy to see that for $m_z \sim 1$ then $\lambda \rightarrow \infty$ (we could as well consider $m_z \sim -1$ of course, and the result would be the same) so we restrict our considerations to $|m_z| \simeq 1$. Simplifying the expression of ψ we have

$$\psi(\lambda) = \frac{e^{\lambda}}{2\lambda},$$

and inverting Eq. (9):

$$\lambda = \frac{1}{1 - m_z} \equiv \frac{1}{\delta}.$$

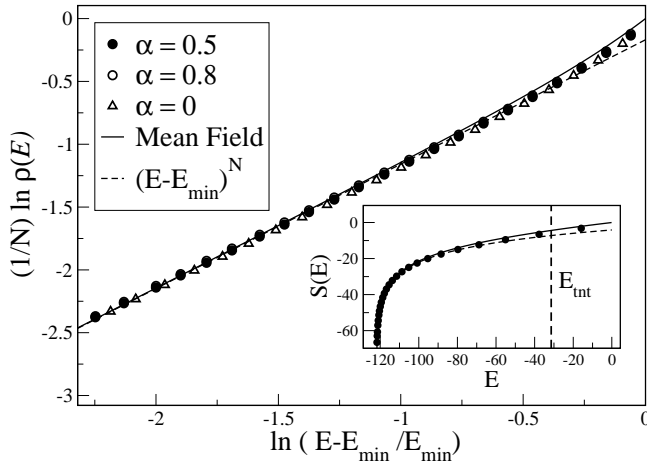


FIG. 4: The specific entropy *vs* energy, obtained numerically for $N = 24$ and different α values (symbols indicated in the legend) is compared with that of the Mean Field Hamiltonian (full curve) and with the power law (dashed line), see Eq. (11). In the inset the entropy is shown *vs* the energy for the case $N = 24$, $\alpha = 0.5$.

From Eq. (8) we obtain:

$$s(\delta) = \ln \delta + \text{const.} = \ln \left(\frac{e - e_{\min}}{-e_{\min}} \right) + \text{const.}, \quad (10)$$

since

$$e = -Jm_z^2 \simeq -J(1 - 2\delta) = e_{\min} + 2\delta J,$$

and $e_{\min} = -J$. From that we immediately have that at low energy,

$$\rho(E) \simeq (E - E_{\min})^N. \quad (11)$$

The next leading order in δ can be calculated from

$$e = -Jm_z^2 = -J(1 - \delta)^2,$$

so that

$$\delta = 1 - \sqrt{-\frac{e}{J}},$$

and

$$s(e) = \ln \left(1 - \sqrt{-\frac{e}{J}} \right) + \text{const.} \quad (12)$$

It is immediate to see that Eq. (12) gives Eq. (10) for $e \simeq e_{\min}$. We compared this analytical result for the Mean-Field model with the DOS computed numerically for the full Hamiltonian (1) and different α values in Fig. 4. The DOS has been calculated using a modified

Metropolis algorithm introduced in [23]. The idea behind is performing a random walk in phase space within an energy range defined by the system temperature. The probability $P(E, T)$ of visiting a configuration with energy E and temperature T , obtained keeping a histogram of the energy values found during a Metropolis run, is related to the DOS through the Boltzman factor $\exp(-E/T)$. That provides us a conceptually simple way of determining the DOS. However, due to finite run time, $P(E, T)$ will only contain information near $\langle E \rangle$ and we must combine the results for runs at different temperatures to obtain the complete DOS over the entire energy range.

As one can see in Fig. 4 the entropy per particle, in the long range case, is almost independent of the range of the interaction, also confirming a result obtained in [25]. Moreover, the theoretical approach gives a very good approximation of the entropy per particle at low energy. When the energy is increased, the first term in the full Hamiltonian (1) becomes important and some deviations appear (see for instance the upper right corner in Fig. 4). Needless to say the excellent agreement confirms the power law behavior for the DOS, Eq. (11), even for energy values sufficiently high. As an example in the inset of Fig. 4, we can see that the power law expression (11) holds up to E_{tnt} .

IV. MAGNETIC REVERSAL TIME

Since the TNT has been introduced for isolated systems, question arises if and how it can be defined when the system is in contact with a thermal bath. From the theoretical point of view we might expect that due to thermal noise the magnetization will be able, soon or later, to change its sign at any temperature T , thus suppressing the ergodicity breaking found in isolated systems. Therefore, strictly speaking, a critical temperature below which the phase space is topologically disconnected for open finite systems does not exist.

Nevertheless we are here interested in more practical questions, for instance: Will the energy threshold E_{tnt} still determine the magnetic reversal time in presence of temperature as it does in isolated chaotic systems? Can we predict the dependence of reversal time from temperature or any other system parameters, like the number of particles?

Since the system is in contact with a thermal bath we may consider it as a member of a canonical ensemble. We may properly define the probability density to have a certain energy value E at the temperature T : $P(E, T)$. Considering all members of the ensemble as independent objects we may guess that when the average energy $\langle E \rangle$ is much less than E_{tnt} and the probability density $P(E, T)$ sufficiently peaked around its average value, the majority of the members of the ensemble will not cross the barrier, or at least, the probability of crossing it will be small. On the other hand for mean energy $\langle E \rangle$ on the order of E_{tnt} each member will be allowed to jump, with a

time essentially given by the microcanonical expression Eq. (5).

Let us further assume, following the standard fluctuation theory [10, 16], that the magnetic reversal times between states with opposite magnetization are determined by the free energy barrier ΔA between states at the most probable magnetization and states with zero magnetization:

$$\tau \propto \exp\left(\frac{\Delta A}{T}\right) = \frac{\text{Max}_m[P_T(m)]}{P_T(m=0)}, \quad (13)$$

where

$$P_T(m) = \exp[-A(T, m)/T],$$

is the probability density to have magnetization m at the temperature T . Since $\text{Max}_m[P_T(m)]$ is usually a slow varying function of the temperature, we can write

$$\tau \propto \frac{1}{P_T(m=0)}.$$

The crucial point now, is to obtain such value using the microcanonical results obtained in the previous Section, namely:

$$P_T(m=0) = \frac{1}{Z_T} \int P_E(m=0) e^{-E/T} \rho(E) dE, \quad (14)$$

where $\rho(E)$ is the density of states and

$$Z_T = \int e^{-E/T} \rho(E) dE, \quad (15)$$

is the partition function. Since $P_E(m=0) = 0$ for $E < E_{\text{tnt}}$, the ergodicity breaking acts as a cut-off energy of the integral (14), so that if the average energy is well below E_{tnt} we can expect very large average reversal times.

In order to verify that Eq. (14) actually gives the magnetic reversal time, we simulated the dynamics of a spin system in contact with a thermal bath in two different ways, the Metropolis algorithm [20], and using the stochastic differential equations of the Langevin type as suggested in [21].

In the Metropolis dynamics the change in the spin direction has been taken at each step completely random on the unit sphere while in the Langevin approach a small dissipation has been added. We checked that the results are independent of such dissipation and that the two approaches give the same results.

Obviously, both approaches can give directly the distribution function: $P_T(m=0)$, but we prefer here the direct calculation of the density of states and thus the possibility to get $P_T(m=0)$ for any temperature[23], with less numerical effort and greater reliability. As for the reversal time it is quite obvious that an arbitrary multiplicative factor should be considered when the two

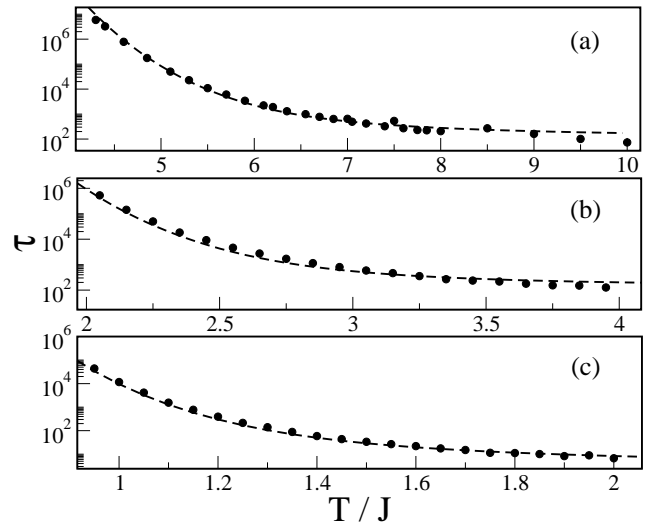


FIG. 5: Average reversal time τ as a function of the rescaled temperature T/J for different interaction range. a) all-to-all $\alpha = 0$, $N = 24$; b) long-range case $\alpha = 0.5$, $N = 24$; c) critical-case, $\alpha = 1$, $N = 20$. Circles are numerical data, dashed line is the integral calculated in Eq. (14).

different approaches are compared (the unit of time in the Metropolis approach is given by a random spin flip).

Results are shown in Fig. 5 where the average reversal time (obtained with the Metropolis dynamics) *vs* the rescaled temperature T/J has been considered for different α and N values as indicated in the caption. As one can see the agreement between the integral (14) (dashed line in Fig. 5) and the numerical results (full circles) is excellent over 4 order of magnitude. It is worth of mention that no parameter fitting, other than a multiplicative constant has been used.

It is also remarkable that a small variation in the temperature scale (about a factor 2) generates a huge variation of the average time (roughly 3-4 orders of magnitude). This signals an exponential dependence by the inverse temperature. Nevertheless a simple temperature dependence cannot be found in general, even if all curves in Fig. 5 can be fitted by the function $T^a \exp(b/T)$, with a and b fitting parameters.

The exponential $1/T$ dependence can be understood in the limit of low temperature. Unfortunately we cannot compute directly the average time for temperatures lower than those shown, due to computer capability, even though we can study the asymptotic behavior of the integral (14) for low temperature.

In order to obtain the low temperature behavior of the magnetic reversal times, we can use the saddle point

approximation to Eq. (14) getting:

$$P_T(m=0) \simeq P_{E^*}(m=0) e^{(\langle E \rangle - E^*)/T} e^{S(E^*) - S(\langle E \rangle)}, \quad (16)$$

where $\langle E \rangle$ and E^* are given by:

$$\frac{1}{T} = \frac{dS}{dE}(\langle E \rangle) = \frac{ds}{de}(e), \quad (17)$$

where $S = \ln \rho$, and

$$\frac{1}{T} = \frac{dS}{dE}(E^*) + \frac{N}{E^* - E_{tnt}} \quad (18)$$

where we used $P_{E^*}(m=0) \propto (E^* - E_{tnt})^N$, see Sect. II. An approximate expression for (17) and (18) can be obtained for small temperature. Indeed, using for the entropy the expression Eq. (12) obtained in Sect. III, and inverting Eq. (17), one obtains:

$$\frac{e}{e_{min}} = \frac{1}{2} \left(1 + \frac{T}{e_{min}} + \sqrt{1 + \frac{2T}{e_{min}}} \right), \quad (19)$$

so that, for $T \ll |e_{min}|/2$, we get:

$$\langle E \rangle = E_{min} \left[1 + \frac{NT}{E_{min}} + O\left(\frac{NT}{E_{min}}\right)^2 \right]. \quad (20)$$

In the same way Eq. (18) can be written as:

$$E^* = E_{tnt} + NT \left[1 + \frac{NT}{\Delta} + O\left(\frac{NT}{\Delta}\right)^2 \right], \quad (21)$$

where $\Delta = E_{tnt} - E_{min}$ and, for temperature sufficiently low,

$$T \ll T_{cr} = \frac{E_{tnt} - E_{min}}{2N} < \frac{e_{min}}{2}, \quad (22)$$

we have

$$E^* = E_{tnt} + NT.$$

Eq. (16) can be further simplified, using the approximated expressions for $\langle E \rangle$ and E^* obtained above and Eq. (11) for the DOS:

$$\begin{aligned} S(E^*) &\simeq N \ln(\Delta + NT), \\ S(\langle E \rangle) &\simeq N \ln NT, \\ P_{E^*}(m=0) &\simeq (E^* - E_{tnt})^N \simeq (NT)^N. \end{aligned} \quad (23)$$

Finally, neglecting terms of order (NT/Δ) :

$$\tau \sim \frac{1}{P_T(m=0)} \sim \exp\left(\frac{E_{tnt} - E_{min}}{T}\right). \quad (24)$$

Even if Eq. (24) has been obtained for low temperature ($T \ll T_{cr}$), it should be kept in mind that this is a classical model so that for $T \rightarrow 0$, when quantum effects become important, it loses its validity[18].

The law (24) has been checked numerically in Fig. 6 where the integral (14) has been calculated for very low temperature and compared with the true exponential law. As one can see asymptotically they are very close over many order of magnitude.

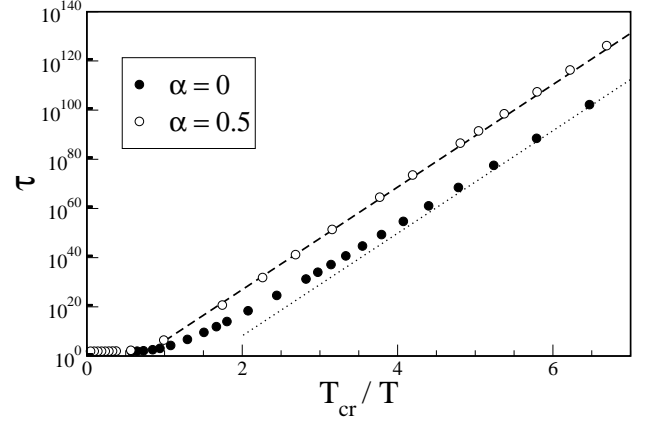


FIG. 6: Average reversal time τ calculated from Eq. (14) as a function of the rescaled temperature T_{cr}/T for different inter-connection range $\alpha = 0$ (full circles) and $\alpha = 0.5$ (open circles) and $N = 24$. Dashed and dotted lines represent their asymptotic value, as given by Eq. (24).

Eq. (24) represents the central result of this paper. Indeed it allows to compute directly the reversal time in presence of a thermal bath at low temperature T without any complicated statistical calculations but the knowledge of the Hamiltonian itself. Moreover, the calculation of both the ground state energy and the Topological Non-connectivity Threshold constitutes a mechanical problem and they can be easily estimated even for complicated models.

Furthermore, it also has some suggestive interpretation. If we consider the path followed by the magnetization, as a random path of a Brownian particle between two potential wells separated by a potential barrier ΔU , according to Kramer's theory [17, 19] the average transition time between the two wells follows the Arrhenius law:

$$\tau \sim \exp(\Delta U/T).$$

Therefore it is clear that the disconnected energy region $\Delta = E_{tnt} - E_{min}$ can be thought of as the real potential barrier felt by the magnetization.

In same way, the critical temperature T_{cr} has the physical meaning of the specific energy barrier. It is interesting to note that the condition $T \ll T_{cr}$ is not too restrictive, at least for long-range systems. Indeed, taking into account that for large N [4]:

$$T_{cr} = r \frac{|E_{min}|}{2N} \simeq \frac{2 - 2^\alpha}{2(2 - \alpha)(1 - \alpha)} N^{1-\alpha},$$

only at criticality ($\alpha = 1$) it does not depend on N (and $T_{cr} = \ln 2$), while generally it grows with the number of particles. This is not at all surprising for a long range systems; indeed, if we make the energy of the system extensive, (multiplying the Hamiltonian by $N/|E_{min}|$), we have $T_{cr} = r/2$, which is finite for any interaction range.

Last, but not least, let us remark that the model given by Hamiltonian (1) at criticality ($\alpha = 1$) is very interesting. Indeed, for $\alpha = 1$ the parameter r (the ratio between the disconnected portion of energy space compared to the full one) goes to zero in the thermodynamical limit. The difference with the short range case is that it goes to zero logarithmically, instead of a power law: $r \sim 1/\ln N$. This simply means the existence of an effective phase transition for finite systems at criticality.

V. CONCLUSIONS

In conclusion we have shown that signatures of the topological disconnection persist when a long range interacting spin system is put in contact with a thermal bath. More precisely for temperature sufficiently low we recover the Arrhenius law for the magnetization reversal time $\tau \propto \exp(\Delta/T)$ similar to the reversal time for a Brownian particle jumping across a potential barrier $\Delta = E_{tnt} - E_{min}$. In other words the magnetization behaves as a stochastic variable and the potential barrier is exactly given by the energy distance between E_{tnt} and E_{min} . This proves the exponential dependence of the reversal times from the number of particles and *stable* ferromagnetism even for small systems with long range interaction and room temperature. The results presented in this paper can be experimentally verified, using for instance the physical system discussed in [15], or in a 3-D spin system with dipole interactions.

We acknowledge useful discussion with J. Barré and S. Boettcher. Financial support from PRIN 2005 and from grant 0312510, DMR division of the NSF is also acknowledged.

-
- [1] D. C. Mattis, *The Many-Body Problem: An Encyclopedia of Exactly Solved Models in One Dimension*, World Scientific Pub Co (1992).
 - [2] F. Borgonovi, G. L. Celardo, M. Maianti, E. Pedersoli, J. Stat. Phys. **116**, 516 (2004).
 - [3] G. Celardo, J. Barré, F. Borgonovi, and S. Ruffo, Phys. Rev. E **73**, 011108 (2006).
 - [4] F. Borgonovi, G. L. Celardo, A. Musesti, R. Trasarti-Battistoni, and P. Vachal, Phys. Rev. E **73**, 026116 (2006).
 - [5] D. Mukamel, S. Ruffo, and N. Schreiber, Phys. Rev. Lett. **95**, 240604 (2005).
 - [6] R. G. Palmer, Adv. in Phys. **31**, 669 (1982).
 - [7] E. du Tremolet de Lacheisserie, D. Gignoux, M. Schlenker, *Magnetism: Fundamentals*, First Springer Science+Business Media, New York (2005).
 - [8] T. Dauxois, S. Ruffo, E. Arimondo, M. Wilkens Eds., Lect. Notes in Phys., **602**, Springer (2002).
 - [9] E. M. Chudnovsky and J. Tejada, *Macroscopic Quantum Tunneling of the Magnetic Moment*, Cambridge Univ. Press, Cambridge (1998).
 - [10] R. B. Griffiths, C. Y. Weng, and J. S. Langer, Phys. Rev. **149**, 1 (1966).
 - [11] P. Gambardella et al., Nature **146**, 301 (2002).
 - [12] A. Vindigni, A. Rettori, M. G. Pini, C. Carbone, P. Gambardella, Appl. Phys. A **82**, 385 (2006).
 - [13] Y. Li and B-G. Liu, Phys. Rev. B **73**, 174418 (2006).
 - [14] L. Cai et al., Phys. Rev. Lett. **79**, 4361 (1997); L. Casetti et al., Phys. Rep. **337**, 237 (2000); R. Franzosi, M. Pettini, Phys. Rev. Lett. **92**, 060601 (2004); R. Franzosi, M. Pettini, L. Spinelli, Nucl. Phys. B **782**, 189 (2007); R. Franzosi, M. Pettini, Nucl. Phys. B **782**, 219 (2007); L. Casetti, M. Pettini, and E. G. D. Cohen, J. Stat. Phys. **111**, 1091 (2003).
 - [15] A. Campa, R. Khomeriki, D. Mukamel, S. Ruffo, Phys. Rev. B **76**, 064415 (2007).
 - [16] L. D. Landau, E. M. Lifshitz, L. P. Pitaevskii, *Statistical Physics*, Pergamon Press, Oxford (1980).
 - [17] H. A. Kramers, Physica **7**, 284, (1940).
 - [18] Classical spin models can be applied only when the temperature T is sufficiently larger than some characteristics quantum energy $\hbar\omega_0$.
 - [19] P. Hanggi, P. Talkner, M. Borkovec, Rev. Mod. Phys. **62**, 2 (1990).
 - [20] N. Metropolis, A. W. Rosenbluth, M. N. Rosenbluth, A. H. Teller and E. Teller. J. Chem. Phys. **21**, 1087, (1953).
 - [21] V. P. Antropov, S. V. Tretyakov and B. Harmon, J. Appl. Phys. **81**, 3961 (1997).
 - [22] D. P. Landau, Shan-Ho Tsai, and M. Exler, Am. J. Phys. **72**, 1294 (2004).
 - [23] J. Hove, Phys. Rev. E **70**, 056707 (2004).
 - [24] J. Barre, F. Bouchet, T. Dauxois and S. Ruffo, J. Stat. Phys. **119**, 677 (2005).
 - [25] R. Salazar, R. Toral and A. R. Plastino, Physica A **305**, 144 (2002).